OPEN ACCESS

University of BRISTOL

Coulter, P., Grubb, M. P., Koyama, D., Sazanovich, I. V., Greetham, G. M., & Orr-Ewing, A. J. (2015). Recombination, Solvation and Reaction of CN Radicals Following Ultraviolet Photolysis of ICN in Organic Solvents. *Journal of Physical Chemistry A*, *119*(52), 12911-12923. https://doi.org/10.1021/acs.jpca.5b10716

Peer reviewed version

License (if available):
Unspecified

Link to published version (if available):
10.1021/acs.jpca.5b10716

Link to publication record in Explore Bristol Research
PDF-document

This document is the Accepted Manuscript version of a Published Work that appeared in final form in Journal of Physical Chemistry A, copyright © American Chemical Society after peer review and technical editing by the publisher. To access the final edited and published work see DOI: 10.1021/acs.jpca.5b10716.

University of Bristol - Explore Bristol Research
General rights

This document is made available in accordance with publisher policies. Please cite only the published version using the reference above. Full terms of use are available:
http://www.bristol.ac.uk/red/research-policy/pure/user-guides/ebr-terms/

Recombination, Solvation and Reaction of CN radicals Following Ultraviolet Photolysis of ICN in Organic Solvents

Philip Coulter,[1] Michael P. Grubb,[1] Daisuke Koyama,[1] Igor V. Sazanovich,[2] Gregory M. Greetham[2] and Andrew J. Orr-Ewing[1,*]

[1] *School of Chemistry, University of Bristol, Cantock's Close, Bristol BS8 1TS, UK*

[2] *Central Laser Facility, Research Complex at Harwell, Science and Technology Facilities Council, Rutherford Appleton Laboratory, Harwell Oxford, Didcot, Oxfordshire, OX11 0QX, UK.*

11 December 2015

* Author for correspondence

e-mail: a.orr-ewing@bristol.ac.uk

Phone: +44 (0)117 9287672

KEYWORDS: Time-Resolved Absorption Spectroscopy; Liquid Phase; Solvent Complexes; Recombination; Reaction Dynamics.

ABSTRACT

The fates of CN radicals produced by ultraviolet (UV) photolysis of ICN in various organic solvents have been examined by transient electronic and vibrational absorption spectroscopy (TEAS and TVAS). Near-UV and visible bands in the TEAS measurement enable direct observation of the CN radicals and their complexes with the solvent molecules. Complementary TVAS measurements probe the products of CN-radical reactions. Geminate recombination to form ICN and INC is a minor pathway on the 150 fs – 1300 ps timescales of our experiments in the chosen organic solvents; nonetheless, large infra-red transition dipole moments permit direct observation of INC that is vibrationally excited in the C≡N stretching mode. The time constants for INC vibrational cooling range from 30 ps in tetrahydrofuran (THF) to 1400 ps in more weakly interacting solvents such as chloroform. The major channel for CN removal in the organic solvents is reaction with solvent molecules, as revealed by depletion of solvent absorption bands and growth of product bands in the TVA spectra. HCN is a reaction product of hydrogen atom abstraction in most of the photo-excited solutions, and forms with vibrational excitation in both the C-H and C≡N stretching modes. The vibrational cooling rate of the C≡N stretch in HCN depends on the solvent, and follows the same trend as cooling rate of the C≡N stretch in INC. However, in acetonitrile solution an additional reaction pathway produces $C_3H_3N_2^{\bullet}$ radicals, which release HCN on a much longer timescale.

1. INTRODUCTION

The ultraviolet photolysis of ICN is an extensively studied process which has been used to explore nuclear dynamics in electronically excited states and bimolecular reactions of the photofragment CN radical. The dissociation of the I-CN bond in isolated, gas-phase ICN molecules has been directly observed on the femtosecond timescale,[1-3] and computational and experimental studies characterized the dissociative electronic potentials[4-6] and the resulting quantum-state specific I and CN energy distributions.[7-35] The ultraviolet absorption of gaseous ICN peaks at wavelengths around 250 nm, with the broad absorption band structure composed of excitations from the linear $^1\Sigma^+_0$ ground state to excited states of $^1\Pi_1$, $^3\Pi_{0+}$ and $^3\Pi_1$ symmetry. The $^3\Pi_{0+}$ state correlates asymptotically with CN ($X^2\Sigma^+$) radicals and spin-orbit excited I*($^2P_{1/2}$) atoms, but a conical intersection with the $^1\Pi_1$ state provides a non-adiabatic pathway to the lower-lying CN ($X^2\Sigma^+$) + I($^2P_{3/2}$) asymptote.[4] This conical intersection is accessed within ~30 fs, and the dynamics of passage through the conical intersection induce high degrees of rotational excitation in the CN radical.

The suggestion by Benjamin and Wilson that ICN would provide a model system for the study of solution phase dynamics[36] has precipitated numerous experimental studies of the chemical dynamics of ICN photolysis in liquids using ultrafast transient absorption spectroscopy.[37-42] The interpretation of these experimental measurements has been supported by simulations of the dissociation dynamics and fates of the I and CN fragments.[41, 43-49] Rivera *et al*.[39] reported a peaked feature centred at 390 nm in the UV/visible absorption spectrum after photolysis of ICN in water and ethanol that closely resembled a low resolution gas-phase *B*←*X* spectrum of the CN radical. This peak was assigned to free, unsolvated CN radicals, and rapidly evolved into significantly broader spectral features peaking at 326 nm in water and 415 nm in ethanol which correspond to solvated radical species. A combination of these experimental

measurements and dynamics simulations using the potential energy surfaces of Morokuma and co-workers[4, 6] showed that CN and I radicals will undergo recombination as a result of the solvent cage in ~60 fs and diffusive recombination in ~16 ps.[39] Furthermore Bradforth and co-workers demonstrated that nascent, rotationally hot CN radicals will retain their rotational coherence for up to a few picoseconds in solution.[38, 49] The photochemistry of ICN has also been studied in cryogenic matrices, with Fraenkel and Haas assigning an infrared band that developed to lower wavenumber than the ICN fundamental C≡N stretching mode to the INC isomer.[50]

In addition to recombination, CN radicals produced through photolysis in solution may undergo bimolecular reactions.[51-53] Hochstrasser and coworkers were the first to apply transient infrared absorption spectroscopy to observe the production of HCN and DCN in chloroform and d-chloroform on ultrafast timescales.[54] Further studies by Crowther *et al*.[55-56] identified the role played by CN radical complexes with chlorinated solvents, while Orr-Ewing and co-workers observed mode-specific vibrational excitation of the C-H stretching and bending modes of HCN products of CN-radical reactions, and their subsequent cooling by coupling to the solvent bath.[41-42, 48, 57-58]

The current study combines ultrafast transient absorption spectroscopy in the UV/visible and infrared spectral regions to observe the initial solvation of CN radicals from ICN photolysis, and the competition between geminate recombination to form ICN and the isomeric INC, solvent-complex formation, H-atom abstraction reactions, and addition reactions with solvent molecules. We report observations following ICN photolysis in chloroform, dichloromethane (DCM), acetonitrile, tetrahydrofuran (THF), methanol and ethanol, providing a comprehensive picture of the various fates of photo-produced CN radicals in solution on femtosecond to picosecond timescales.

2. EXPERIMENTAL DETAILS

Ultrafast transient absorption spectroscopy measurements used both the ULTRA laser system, at the Central Laser Facility of the Rutherford Appleton Laboratory, and a femtosecond laser system at the University of Bristol. Detailed descriptions of the laser-based instruments and the sample preparation and handling procedures are presented elsewhere,[58-60] and we provide only a brief summary here.

Transient vibrational absorption spectroscopy (TVAS) experiments were conducted with 0.29 M solutions of ICN (98%; Acros Organics) and BrCN (Aldrich; 97%) which were prepared in acetonitrile (Fisher Chemical; 99%), dichloromethane (VWR Chemicals; >99%, with 0.2% ethanol), chloroform (VWR-Chemicals, >99%), tetrahydrofuran (VWR, 99.5%), and d-acetonitrile (Sigma Aldrich; 99.8% D). All hydrogenated solvents were dried using 3 and 5 Å zeolite molecular sieves. ICN was recrystallized from toluene (Sigma-Aldrich Analytical Grade) before use. Sample volumes of 5 – 10 ml were circulated through a Harrick cell using a peristaltic pump and PTFE tubing. The Harrick cell was fitted with CaF_2 windows separated by 380 μm.

ICN was photolysed using a UV pump pulse (approximate duration: 50 fs ULTRA; 120 fs Bristol) with a wavelength of 267 nm. The pump pulses were delivered to the liquid samples at repetition rates reduced to half the laser output frequency (output frequency: 10 kHz ULTRA; 1 kHz Bristol) using a mechanical chopper. For TVAS measurements, IR pulses at the laser output frequency were overlapped spatially with the UV pulses at the sample. A motorized translation stage varied the length of the path followed by the UV laser pulses to set the time delays between UV pump and IR probe pulses. Delays were selected in a random order and were controlled with sub-picosecond time resolution and maximum values of up to

3000 ps (ULTRA) and 1300 ps (Bristol). The IR laser pulse wavelength was centred near 2100 cm^{-1}, and had an approximate bandwidth of 500 cm^{-1} (ULTRA) or 300 cm^{-1} (Bristol). IR radiation transmitted through the sample was dispersed onto a 128-element array detector (with mercury cadmium telluride elements) from which averaged spectra were accumulated and processed to determine the wavelength-dependent changes in absorbance induced by the UV pump pulse. Spectra of 1,4-dioxane were used to calibrate the wavelength scale of the TVAS measurements. Subsequent analysis of TVAS data used the KOALA software package.[61]

Transient electronic absorption spectroscopy (TEAS) measurements were made using the Bristol ultrafast laser system. In addition to the samples used for TVAS, the TEAS measurements used 0.29 M solutions of ICN in methanol (Fischer Chemicals, 99.99%) and ethanol (BDH Reagents, Spectroscopy Grade). Approximately 1 μJ/pulse of the fundamental output of an amplified Titanium:Sapphire laser (1 kHz, 40 fs pulse duration) generated white-light continuum (WLC) pulses by focusing into a rastered 5-mm thick CaF_2 window using a 100-mm focal length lens. The recollimated WLC pulses spanned the approximate wavelength range of 320 to 650 nm. Time delays between the UV pump and WLC probe pulses were selected using the same procedure as for TVAS measurements. The near-UV and visible radiation components of the WLC pulses transmitted by the sample were collected into an optical fiber and dispersed onto a 750-pixel CCD spectrometer (Avantes, AvaSpec-DUAL) with a spectral resolution of 0.6 nm. Analysis with the KOALA package[61] corrected spectra for probe-pulse frequency chirp and enabled decomposition into spectral components.

Steady state FTIR spectra of samples before and after UV irradiation identified the positions of the CN stretching bands of ICN and HCN dissolved in the various solvents. The electronic absorption bands of ICN in different solvents were characterized by subtracting steady state UV/vis spectra of the solvent from the corresponding spectra of the ICN solutions.

3. RESULTS AND DISCUSSION

The UV absorption bands of ICN in various solvents were measured by steady state absorption spectroscopy on static samples to identify any solvent-induced shifts and changes to the band profiles. These results are presented first, and compared to the known gas-phase spectrum of ICN.[62] TEAS was then used to observe the production, solvation and loss of CN radicals following ICN photolysis in solution. The fates of these radicals were studied using TVAS in the mid-IR spectral region.

3.1 Steady-State UV Absorption Spectra

The UV absorption bands of ICN are well-characterized in the gas phase but are modified by interaction with solvent molecules. **Figure 1** compares the gas-phase spectrum[63] with spectra obtained in various solvents, for which the solvent-only absorption spectra have been subtracted to isolate the ICN features. The maxima in the solution spectra are shifted to lower wavelength than the gas-phase spectrum, with the shift increasing from chloroform and dichloromethane to acetonitrile, methanol and THF. These spectral shifts have previously been attributed to stabilization of the ground state of ICN, which has a large permanent dipole moment, by polar solvents. To a lesser extent, these solvents also destabilize the electronically excited states of ICN contributing to the broad UV absorption band.[38-39, 47] However, the band maxima do not show a straightforward correlation with either solvent molecular dipole moments or relative permittivities, suggesting a more complex interaction of the solvents with the electronic states of ICN.

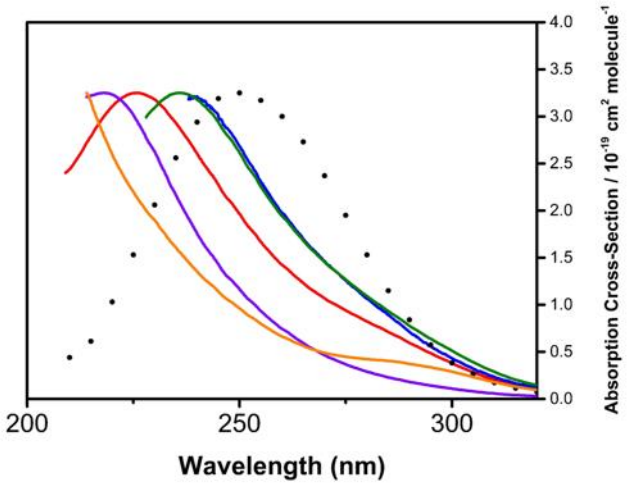

Figure 1: Normalized steady-state UV absorption spectra of ICN in various common solvents. Pure solvent spectra have been subtracted to isolate the contributions from ICN absorption. The solvents are: THF (orange); methanol (purple); acetonitrile (red); chloroform (green); dichloromethane (blue). A gas-phase spectrum is shown by dots, with absorption cross sections on the right-hand axis.

In each case, absorption at 267 nm is on the long-wavelength side of the ICN band and favours excitation to the $^3\Pi_{0+}$ and $^3\Pi_1$ states correlating adiabatically to the I* + CN and I + CN dissociation limits respectively. Although there is a shallow minimum in the $^3\Pi_{0+}$ state (and perhaps also in the $^3\Pi_1$ state), dissociation is prompt (~100 fs) at the excitation energy used.[39]

3.2 TEAS of Photoexcited ICN Solutions

The time-resolved electronic absorption spectra of ICN solutions show transient absorption features across the near-UV and visible regions, and examples are presented in **Figure 2** for five solvents: chloroform (**Fig. 2(a)**), dichloromethane (**Fig. 2(c)**), acetonitrile (**Fig. 2(d)**), ethanol (**Fig. 2(e)**) and methanol (**Fig. 2(f)**). The interpretation of the broad overlapping bands was previously discussed by both Bradforth and co-workers[39] and Keiding and co-workers.[40] Despite this prior analysis, the decomposition of such spectra and the subsequent assignment of component bands to specific molecular species remains a challenge. Nonetheless, ICN

photolysis in chloroform provides a clear separation of some of the observed absorption features; the decomposition of one transient spectrum obtained at a time delay of 1.2 ps is presented in **Figure 2(b)**. The sharp peak centred at 390 nm is assigned to CN radicals which are only weakly solvated by chloroform, resulting in a small shift of the ($B \leftarrow X$) transition from the gas phase absorption centre. We refer to these weakly solvated CN radicals as *free* CN and consider their electronic states to be largely unperturbed by interactions with the solvent. The free CN peak grows rapidly before decaying with a 3.3 ± 1.0 ps time constant; meanwhile, a broad feature peaking at 340 nm grows with a 1.7 ± 0.7 ps time constant before decaying slowly across the experimental time window. One plausible assignment of this feature is to a solvent-to-solute charge transfer (CT) band in which the solute is a ground-state iodine atom (I($^2P_{3/2}$)). The corresponding I*($^2P_{1/2}$) – solvent CT band is shifted to longer wavelength and contributes a broad background to the transient absorption spectra that peaks in the wavelength region above 450 nm. Electronic quenching of the spin-orbit excited I* atoms will reduce the intensity of this broad feature and should cause a commensurate rise in the I($^2P_{3/2}$) – solvent CT band. The time constants for the growth of the 340-nm features are similar in chloroform (1.7 ± 0.7 ps) and dichloromethane (1.1 ± 0.5 ps), but are slightly smaller than the time constants of 2.0 ± 0.4 ps and 1.4 ± 0.5 ps for the initial fast decay of the I*($^2P_{1/2}$) CT band.

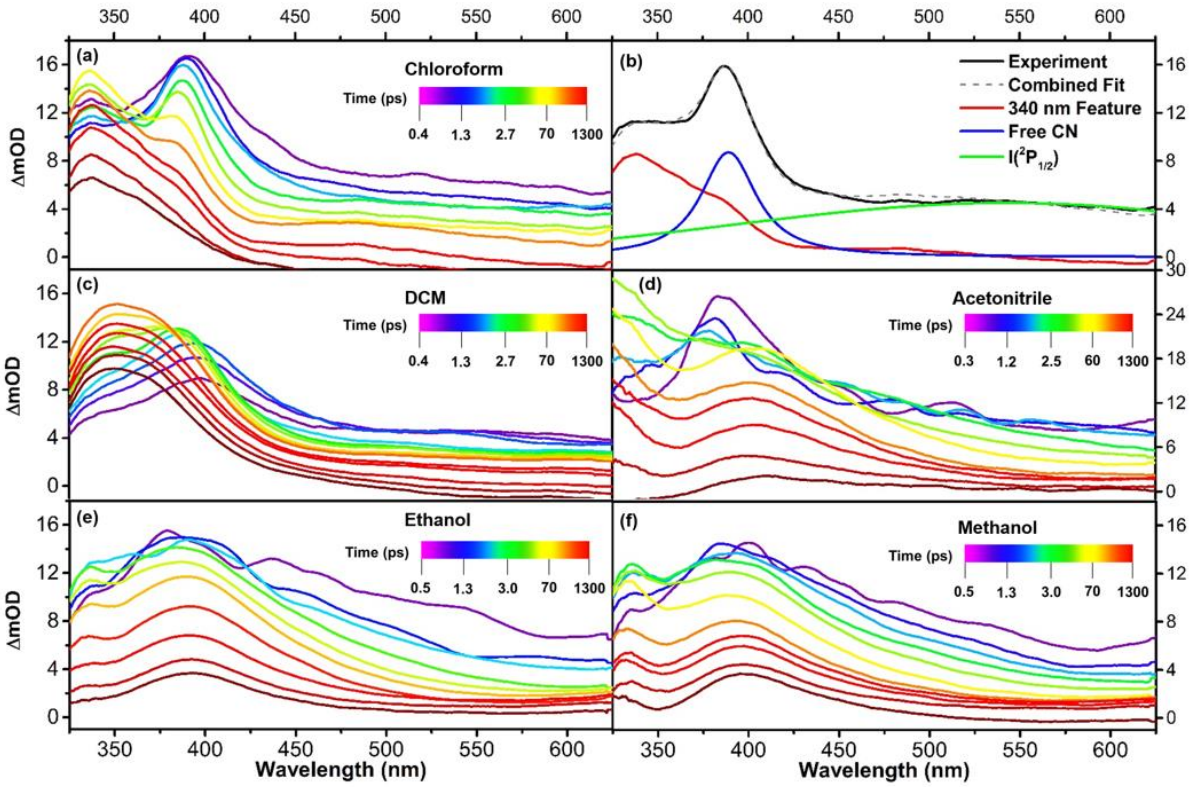

Figure 2: TEAS spectra of ICN photolysis in (a) chloroform, (c) dichloromethane, (d) acetonitrile (e) ethanol and (f) methanol. The various colours from purple to dark red represent spectra obtained at increasing excitation-to-probe laser pulse time delays up to 1300 ps, as indicated by inset keys. Panel (b) provides an example of the decomposition of a transient absorption spectrum obtained in chloroform at a single time delay of 1.2 ps. In the decomposition, the feature peaking at 340 nm (red line) has contributions from both solvent-to-solute I($^2P_{3/2}$) CT and CN-radical complex absorption bands. The shape of this feature is taken from a late time spectrum for ICN photolysis in chloroform. The feature centred at 390 nm (blue line) is a Lorentzian function that represents free CN-radical absorption, and the broad feature centred at 540 nm is a Gaussian function representing solvent-to-solute I*($^2P_{1/2}$) CT. Similar contributions to the TEA spectra can be identified for the measurements made in acetonitrile and dichloromethane, but are less distinct in ethanol and methanol where the broad feature representing I($^2P_{3/2}$) CT and CN-radical complex absorption peaks between 375 and 395 nm.

Bradforth and co-workers[39] proposed that following ICN photolysis in water, a broad solvated-CN absorption feature overlaps the I($^2P_{3/2}$) CT band in the near UV, with the two spectral features being difficult to distinguish. Much of the absorption observed in our TEA spectra at near-UV wavelengths and extending to the visible may therefore be associated with solvated forms of the CN radical. The shift of the CN absorption to shorter wavelengths as a result of solvation has been quantified theoretically by Pieniazek *et al.*[64] The smaller blue shift of the

CN absorption in ethanol than in water is attributed to ethanol's lower dipole moment. The broad near-UV feature cannot be assigned uniquely to an $I(^2P_{3/2})$ - solvent CT band or solvated CN on the basis of our spectroscopic observations; instead, both species are likely to contribute to the absorption at 340 nm, and hence to the time constant for its growth. The low dipole moments of chlorinated solvents and acetonitrile compared to water do not obviously account for the spectral position of the solvated CN bands to the blue of the free CN ($B \leftarrow X$) absorption; instead, strong complexing interactions of CN-radicals with individual solvent molecules are thought to be responsible, as proposed by Crowther *et al*.[55-56]

We explored the spectra of CN-solvent complexes in chloroform, dichloromethane and acetonitrile further by computational methods. Density functional theory (DFT) calculations were used to optimise the structures of the complexes, and time-dependent DFT (TD-DFT) calculations predicted CT absorptions peaking at 336 nm, 330 nm and 294 nm for CN-chloroform, CN-DCM and CN-acetonitrile complexes (see the **Supporting Information**). These calculations were performed using the Gaussian 09 package[65] with the unrestricted CAM-B3LYP functional and an aug-cc-pVTZ basis set. The calculations are in reasonable agreement with experimental observations for CN-chloroform and CN-dichloromethane TEA spectra, and the prediction of a shorter absorption wavelength for the CN-acetonitrile complex accords with the spectra shown in **Fig. 2(d)**. The peak of the CN-acetonitrile absorption lies further into the UV than the extent of our white-light continuum, but the long-wavelength wing of this band is observed.

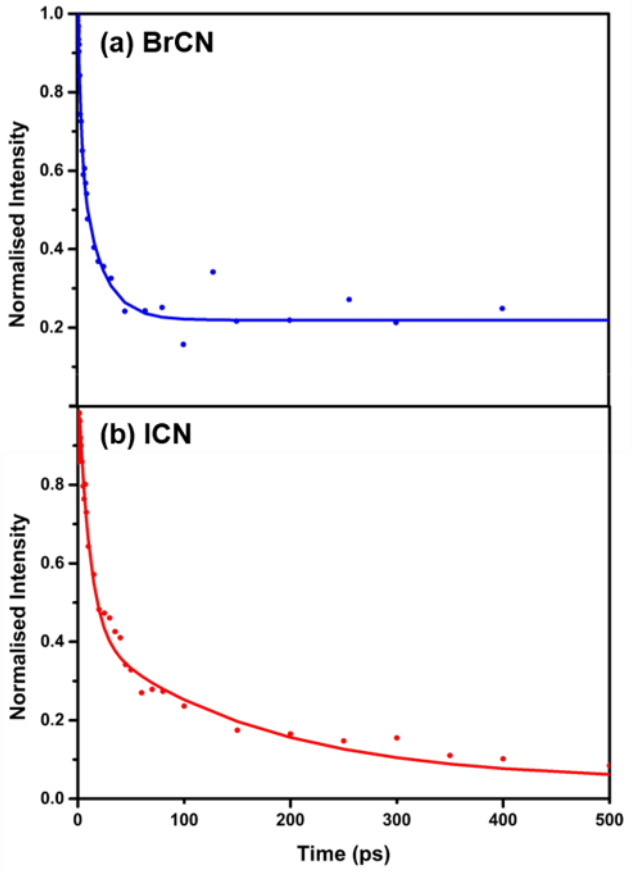

Figure 3: Normalized intensity of the broad feature peaking at 340 nm plotted as a function of time (dots) after (a) BrCN and (b) ICN photolysis in acetonitrile solution. The intensities were fitted with a single exponential decay for BrCN (blue line) and a double exponential decay for ICN (red line).

Further resolution of the chemical identities of the species responsible for the 340-nm band comes from comparative studies of BrCN and ICN photolysis in acetonitrile solution. The same broad near-UV absorption band is observed when ICN is preplaced by BrCN, indicating an assignment to solvated CN radicals, but Br-solvent CT bands cannot be immediately discounted. **Figure 3** compares the time dependence of the intensity of the 340-nm feature after BrCN (**Fig. 3(a)**) and ICN (**Fig. 3(b)**) photolysis in acetonitrile. The 340 nm feature decays to 20 % of the band maximum after BrCN photolysis, with a single exponential time constant of 11 ± 2 ps which is similar to the 9.8 ± 1.5 ps initial time constant measured after ICN photolysis. The longer component of the decay evident after ICN photolysis (with time constant of 158 ±

25 ps) is not observed after BrCN photolysis, and is therefore assigned to the I($^2P_{3/2}$) - solvent CT band. The longer-lived, but weak absorption observed for the BrCN solution is suggested to be a signature of the corresponding CT band for Br – acetonitrile complexes. The faster decay seen in both measurements most likely corresponds to loss of solvated CN-complexes, which undergo reaction or geminate recombination with an ~10 ps time constant.

TEAS measurements subsequent to ICN photolysis in dichloromethane show similar spectral features to those observed in chloroform. However, the band assigned to free CN is only visible at the earliest time delays in acetonitrile, ethanol and methanol; for these solvents, the spectra are dominated by broad absorption bands. The photochemistry of ICN in acetone was discussed recently,[66] and shows many of the features described above, but an additional band centred below 350 nm was observed that was assigned to absorption from the lowest triplet state of acetone.

The 340-nm band does not return to the baseline within the 1300 ns timescale of the experimental measurements in any of the organic solvents studied, but does disappear in water where fast radical recombination dominates.[39] Although the reaction of CN radicals with solvent molecules to make HCN may be relatively slow in chlorinated solvents,[55-56] in most other organic solvents the CN radicals are expected to react on pico- to nanosecond timescales, producing an organic radical co-product. The corresponding reaction is endothermic by ~ 24.8 kJ mol^{-1} with water,[67] and is therefore unfavourable. Spin-orbit excited I*($^2P_{1/2}$) atoms will quench rapidly to the ground state I($^2P_{3/2}$) atoms, and these in turn decline steadily in numbers because of diffusive recombination with other I atoms or organic radicals. These I atoms are likely contributors to the late-time 340-nm absorption band as argued above. However, possible overlap of the broad 340-nm band with other spectral features, and uncertainty over the expected shapes and centre wavelengths of the I-solvent and I*-solvent CT bands precluded further interpretation.

Table 1: Time Constants (in ps) for the Growth and Decay of Spectral Bands Observed by TEAS for UV-Excited ICN in Various Solvents.

Solvent	**Time Constant / ps [(a)]**			
	Free CN decay	**340 nm feature growth**	**340 nm feature decay**	**I*($^2P_{1/2}$) – solvent CT band decay**
Acetonitrile	0.6 ± 0.1	0.6 ± 0.1	9.8 ± 1.5, 158 ± 25	
Chloroform	3.3 ± 1.0	1.7 ± 0.7	1500 ± 150	2.0 ± 0.4, 220 ± 20
Dichloromethane	1.1 ± 0.5	1.1 ± 0.5	230 ± 50	1.4 ± 0.5, 190 ± 20
Ethanol			27 ± 3	1.5 ± 0.8
Methanol			23 ± 2	1.5 ± 0.8

(a) The band assignments are shown in Figure 2, and spectral decomposition and time-constant fitting used the KOALA program. Missing values indicate that no band associated with that particular feature was clearly observed. Where two time constants are reported, a bi-exponential decay function was required to fit the changing band intensity with time.

Table 1 summarizes the time constants for growth and decay of species contributing to the TEAS data in the solvents studied. Our time resolution prevents us from observing some of the faster processes reported previously by Rivera *et al*.[39] The TEAS data report on the timescales for removal of CN radicals, but several competing pathways can account for these losses. These pathways are distinguished by the analysis of TVAS data presented in the next section.

3.3 Transient Vibrational Absorption Spectroscopy of Photoexcited ICN Solutions

TVAS of photoexcited ICN in various solvents using broadband mid-IR probe pulses concentrated on the C≡N stretching region around 1900 – 2200 cm^{-1}. Example TVAS data are presented in **Figure 4** for measurements in acetonitrile (**Fig. 4(a)**), d-acetonitrile (**Fig. 4(c)**), DCM (**Fig. 4(d)**), chloroform (**Fig. 4(e)**), and THF (**Fig. 4(f)**). The assignments of bands in

spectra obtained in chlorinated solvents have been considered previously,[42] and provide guidance for interpretation of spectra in other solvents. **Fig. 4(b)** shows an example decomposition obtained after ICN photolysis in acetonitrile, with the analysis performed using the KOALA program.[61] Our rationale for band assignments is explained below, and **Table 2** provides a summary.

The band centred at 2160 cm^{-1} in chloroform, and at 2169 cm^{-1} in DCM is assigned to ICN on the basis of FTIR spectroscopy of steady state solutions, and has a negative intensity (a "bleach" feature) in the transient spectra because of depletion of ICN by the UV photolysis laser. Similar bleaches appear following ICN photo-excitation in each of the solvents considered. These peaks show limited signs of recovery on the timescales of our measurements, indicating that liberated CN mostly avoids geminate recombination with I atoms and is instead removed by processes such as reaction with the solvent molecules. In DCM, the depth of the ICN bleach feature grows with increasing time delay, which might be construed as evidence that unphotolysed ICN is reacting with some of the radical species generated photolytically. However, it is unclear why this process would be specific to experiments in DCM, and a more likely explanation is that a band associated with a short-lived intermediate overlaps the ICN bleach feature.

One expected product of reaction of CN radicals with the solvent is HCN, which contributes an absorption band centred at approximately 2090 cm^{-1} that grows with time. This band is assigned to the fundamental vibrational transition from ν_1=0 $\rightarrow$ ν_1=1 (1_0^1) in HCN, with ν_1 denoting the C≡N stretching vibrational mode. The strong transient absorption feature centred at approximately 2060 cm^{-1} is assigned to the INC isomer of ICN,[41-42, 50, 68] which forms by geminate recombination. Although the band intensity suggests a major product, the transition dipole moment of the C≡N stretching mode of INC is known to be much greater than for ICN in cryogenic matrices;[50, 68] as such, the intensity observed for the INC 1_0^1 transition is consistent

with geminate recombination being a minor pathway for CN removal. Differences in transition dipole moments of this type make it difficult to draw more quantitative conclusions about the yields of products based on the relative intensities of bleach and absorption features in the TVAS spectra.

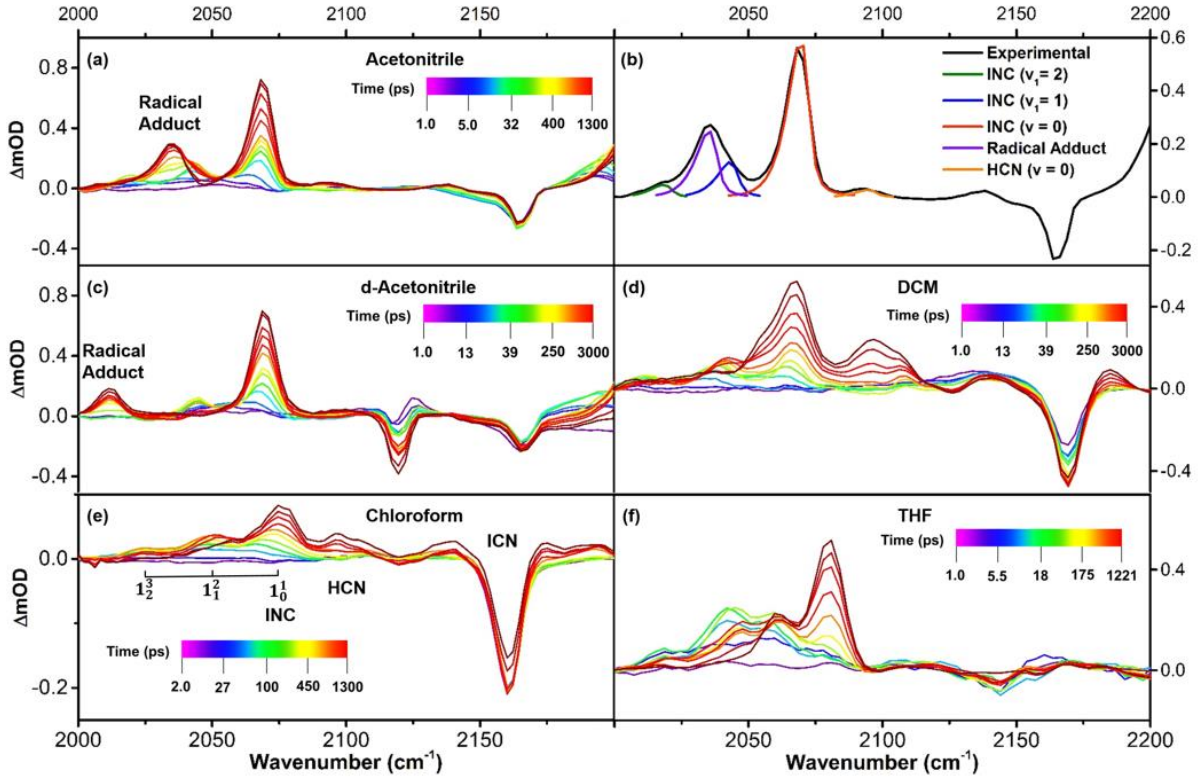

Figure 4: TVAS spectra obtained following ICN photolysis in (a) acetonitrile, (c) d-acetonitrile, (d) dichloromethane, (e) chloroform and (f) tetrahydrofuran. Panel (b) illustrates decomposition of a single time spectrum in acetonitrile and assignment of the constituent absorption features. Each spectral feature is fitted with a skewed Gaussian function which matches the shape of the late-time INC 1_0^1 absorption band unless stated otherwise in the text. Spectra corresponding to individual time delays are represented with different coloured spectra from purple to dark red and show the evolution from reactants to products up to maximum time delays of 3000 ps.

The TVAS data for ICN photolysis in CH_3CN and CD_3CN show some clear similarities to the spectra for the chlorinated solvents as well as some differences. Two weak, sharp bands are evident in the TVAS data for ICN / CH_3CN solutions at 2017 cm^{-1} and 2043 cm^{-1} that are hard to discern from other spectral features for the chlorinated solvents. The 2043 cm^{-1} band also

features in the ICN / CD_3CN spectra, and the 2017 cm^{-1} band may be present but masked by a stronger 2010 cm^{-1} feature. The positions of these two bands, and their time dependence point to an assignment to vibrationally hot INC formed by the geminate recombination of I atoms with CN radicals. The INC v_1=1 ← v_1=0 absorption of the C≡N stretching mode occurs at 2069 cm^{-1}; DFT calculations using the B3LYP functional with a 6-311G** basis set give an anharmonicity constant for the CN stretch of INC of x_{11} = -11.6 cm^{-1}. The v_1=2 ← v_1=1 and v_1=3 ← v_1=2 vibrational hot bands are observed in acetonitrile at 2043 cm^{-1} and 2017 cm^{-1}, indicating an observed anharmonicity constant of x_{11} = -13 cm^{-1} that is consistent with the calculated value. The INC bands shift by approximately 5 cm^{-1} from lower to higher wavenumber in the first 5 ps, which may be a result of nascent excitation in the bending and N-I stretching modes of INC in addition to the C≡N stretch. The calculated anharmonicity constants coupling the bend (x_{12} = -3.4 cm^{-1}) and I-N stretch (x_{13} = -1.6 cm^{-1}) to the C≡N stretching mode of INC support this interpretation. A kinetic model accounting for the production and loss of the vibrationally excited C≡N stretch in INC is presented in section 3.4. TVA spectra of UV-excited ICN / $CHCl_3$ and ICN / CH_2Cl_2 solutions show similar signatures of vibrationally excited INC to the low wavenumber side of the INC fundamental band, although such an assignment does not fully account for the absorptions in this region. The C≡N stretch excited hot bands of INC in the chlorinated solvents are separated by the same anharmonicity constant of x_{11} = -13 cm^{-1} observed in acetonitrile, although the peak positions show different solvent-induced shifts.

An additional bleach of a solvent vibrational band is observed in CD_3CN at 2120 cm^{-1}. The gradual increase in the depth of this feature is attributed to loss of solvent molecules by reaction with CN radicals. The growth in intensity of the bleach can be fitted with a single exponential time constant of 12 ± 3 ps which is more than an order of magnitude slower than the decay of free CN observed in our TEAS studies. The 12 ± 3 ps growth in the CD_3CN bleach therefore

demonstrates that CN reactions with the solvent must have an intermediate step, which we suggest corresponds to formation of CN-solvent complexes. These complexes react more slowly than the timescale for free CN decay, and account for the observed 12 ps CD_3CN removal. The short-time chemistry of CN radicals in acetonitrile is discussed in greater detail in a companion paper.[69]

The HCN 1_0^1 band is not observed in CD_3CN, as expected in the absence of any hydrogenated species, but is only weakly evident in the CH_3CN solutions. The weakness of the HCN 1_0^1 absorption relative to the ICN bleach in acetonitrile solutions, when compared to observations for other solvents, suggests that CN radicals do not react efficiently with acetonitrile to make HCN on these short timescales. However, the development of the 2120 cm^{-1} bleach in the CD_3CN spectra demonstrates that some reaction with the solvent is occurring. These observations can be reconciled if there is an alternative reaction pathway that competes with H/D atom abstraction. The bands at 2036 cm^{-1} in CH_3CN and 2012 cm^{-1} in CD_3CN, labelled as radical adducts in **Figs. 4(a) and 4(c)**, support this interpretation because they have a delayed onset of ~10 ps commensurate with the timescale for the loss of the CN radicals observed by TEAS. The delay suggests that an intermediate to the formation of the species responsible for the 2036 cm^{-1} and 2012 cm^{-1} absorptions in CH_3CN and CD_3CN is a direct result of reaction between the solvent and CN radicals. The spectroscopically observed species subsequently grow with ~30 ps time constants and persist out to the longest timescales measured. *Ab initio* calculations of vibrational frequencies of possible reaction products indicate that the 2036 cm^{-1} band derives from CN-addition to the N or C atom of the nitrile group in acetonitrile to produce a $C_3H_3N_2^{\bullet}$ radical. Possible structures for the CN-acetonitrile radical adduct are discussed elsewhere.[69]

Table 2: Band Centre Wavenumbers Observed in TVA Spectra Obtained in the C≡N Stretching Region Following ICN Photolysis in Five Solvents.

Solvent	**Absorption Band Centre / cm^{-1}** [(a)]								
	ICN $\mathbf{1_0^1}$	Solvent	HCN $\mathbf{1_0^1}$	HCN $\mathbf{1_1^2}$	HCN $\mathbf{1_2^3}$	INC $\mathbf{1_0^1}$	INC $\mathbf{1_1^2}$	INC $\mathbf{1_2^3}$	Radical Adduct
Acetonitrile	2166		2094			2069	2043	2018	2036
d-Acetonitrile	2166	2120				2069	2043	2018	2012
Chloroform	2160		2098			2075	2049	2023	
Dichloromethane	2169		2096			2065	2039	2013	
Tetrahydrofuran			2080	2060	2039	2061			

(a) The spectral resolution of 2.6 cm^{-1} determines the uncertainties in the specified wavenumber values.

The TVA spectra obtained for ICN / THF solutions are strikingly different to those obtained with other solvents. For example, the INC band is weak compared to the HCN 1_0^1 band, the intensity of which is amplified by an enhanced transition dipole moment of HCN in THF (see **Supporting Information**). Furthermore, the INC absorption is overlapped by an absorption centred at 2060 cm^{-1} that we assign to vibrationally hot HCN. This overlapping band grows and decays before the INC 1_0^1 band dominates the absorption, producing a band that peaks at 2061 cm^{-1}. An additional small absorption feature is observed at 2039 cm^{-1} which is also assigned to internally excited HCN. The HCN products of reactions of CN radicals with organic molecules in solution are known to be excited in the C-H stretching (ν_3) and bending (ν_2) modes[41, 58] from TVAS observations in the C-H stretching region around 3200 cm^{-1}. In the gas phase, the couplings of these modes to the C≡N stretch are quantified by anharmonicity constants x_{12} = -3.15 cm^{-1} and x_{13} = -14.9 cm^{-1}.[70] While hot HCN bands in the nitrile region could arise from the 1_0^1 absorption band in otherwise C-H stretch and bend excited HCN, the 2060 and 2039 cm^{-1} band positions observed in the TVA spectra following ICN photolysis in THF agree better with expectations for the 1_1^2 and 1_2^3 hot bands of C≡N stretch excited HCN,

for which the anharmonicity constant is x_{11} = -10.3 cm^{-1}. This assignment is therefore made in Table 2 and we return to it and the analysis of the time dependences of the bands in Section 3.5. An additional band is observed at 2048 cm^{-1} in THF solution; this is not reproducibly present in every data set and its assignment therefore remains uncertain.

3.4 Vibrational Cooling of INC

The TVA spectra reported in Section 3.3 provide evidence that INC is produced vibrationally hot by geminate recombination of the CN and I radicals. The anharmonic shifts predicted by electronic structure calculations point towards excitation of the C≡N stretching mode and we assign the observed bands accordingly, although the other modes are also likely to be excited by formation of the I-N bond.

The INC(v_1) vibrational cooling rates deduced from the decays of the v_1=2 ← v_1=1 and v_1=3 ← v_1=2 hot bands and growth of the fundamental v_1=1 ← v_1=0 absorption band depend strongly on the solvent. The cooling kinetics were treated using a stepwise vibrational cooling model in which only single vibrational quantum changes were considered. The Landau-Teller model of vibrational relaxation predicts that the time constants $\tau_{n\rightarrow(n-1)}$ for the $v = n \rightarrow (n-1)$ steps down a ladder of vibrational levels should scale according to $\tau_{n\rightarrow(n-1)} = {}^{\tau_{1\rightarrow0}}/_{n}$.[71] This expectation was used as a constraint in kinetic fits that used the model shown in Scheme I to describe the INC vibrational cooling. The model assumes that INC can be produced in any of the probed vibrational levels up to v_1 = 2 directly by the recombination reaction. Fits were performed to time-dependent band intensities, which depend on both the population differences between the two vibrational levels connected by an IR transition, and on the increase in transition moments as the vibrational state probed increases. **Figure 5** shows the fits to this model for band intensities measured in acetonitrile (**Fig. 5(a)**), dichloromethane (**Fig. 5(b)**) and

chloroform (**Fig. 5(c)**) solutions, with the derived time constants for vibrational relaxation presented in **Table 3**. The relative magnitudes of the time constants for the association steps derived from the fits account for the relative band intensities and depend inversely on the nascent branching between INC C≡N stretching vibrational levels.

Scheme I

$$\begin{array}{lcl} \text{I + CN} & \xrightarrow{\tau_2} & \text{INC } (v_1 = 2) \\ & & \downarrow \tau_{2\to1} \\ \text{I + CN} & \xrightarrow{\tau_1} & \text{INC } (v_1 = 1) \\ & & \downarrow \tau_{1\to0} \\ \text{I + CN} & \xrightarrow{\tau_0} & \text{INC } (v = 0) \end{array}$$

Table 3: Branching Ratios for the Geminate Recombination to Particular Vibrational Levels of INC and Time Constants for Vibrational Relaxation Steps, Obtained from Fits of TVA Spectral Data to the Kinetic Model of Scheme I.

Solvent	**Recombination Branching Ratio**			**Relaxation Time Constant / ps**	
	INC ($v_1 = 2$)	INC ($v_1 = 1$)	INC ($v_1 = 0$)	$\tau_{2\to1}$	$\tau_{1\to0}$
Acetonitrile	0.08 ± 0.04	0.26 ± 0.04	0.66 ± 0.08	150 ± 23	300 ± 45
Dichloromethane	0.12 ± 0.05	0.32 ± 0.08	0.56 ± 0.13	330 ± 75	660 ± 150
Chloroform	0.12 ± 0.03	0.32 ± 0.05	0.56 ± 0.10	700 ± 120	1400 ± 250

.

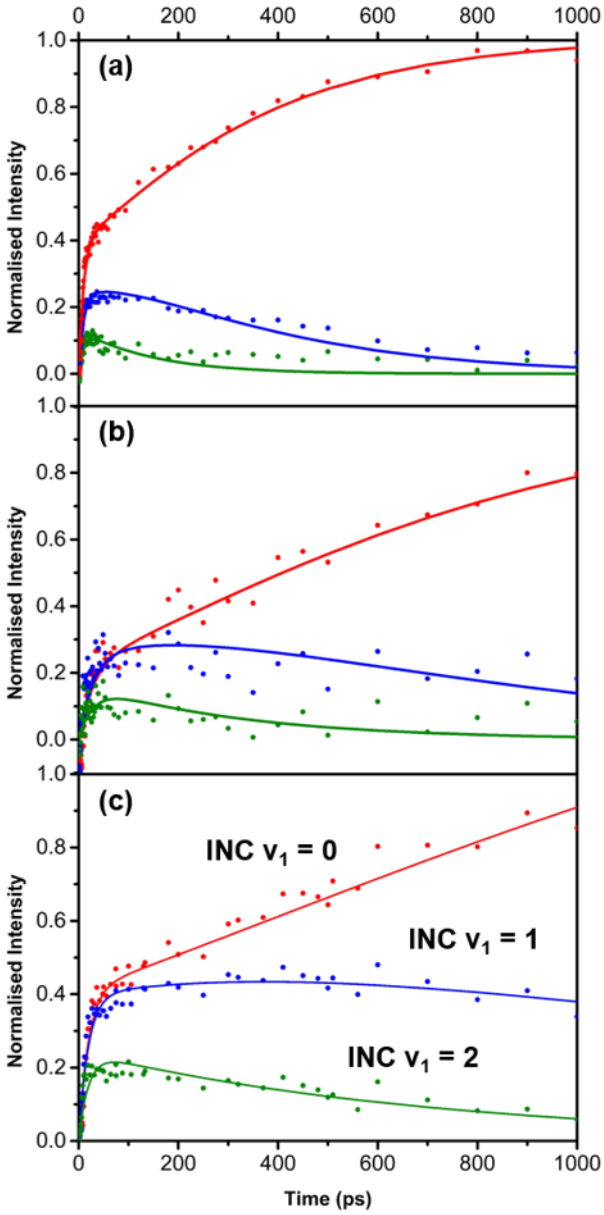

Figure 5: Fits (solid lines) to kinetic Scheme I of the TVAS band intensities (dots) for INC formed through geminate recombination of I and CN for: (a) acetonitrile; (b) dichloromethane; and (c) chloroform solutions. The fitting was performed simultaneously for three bands of INC: red 1_0^1; blue 1_1^2; green 1_2^3.

The recombination timescales derived from the fits presented in **Figure 5** for different INC vibrational levels are summarized in the **Supporting Information**. The combined time constant of 10 ps for recombination in acetonitrile (obtained using $^1/_\tau = \sum_i {}^1/_{\tau_i}$) is consistent with fast decay time constants obtained from the TEA spectra for the 340 nm feature after

BrCN (11 ± 2 ps) and ICN (9.8 ± 1.5 ps) photolysis in acetonitrile. However, given the limited ICN bleach recovery observed in each solvent presented in **Figure 4** and the large transition moment of the ν_1 band of INC, recombination appears to be a minor pathway. The recombination timescales are therefore limited by the faster loss of CN radicals through other channels. Absolute recombination yields are not deduced from the fits to the kinetic model, but the branching ratios to different INC vibrational levels depend inversely on the fitted recombination time constants and are presented in **Table 3**. These branching ratios appear to be insensitive to the choice of solvent for experiments in chloroform, dichloromethane and acetonitrile.

Excitation of the C≡N stretching mode is perhaps surprising given that the new bond formed by geminate recombination is the I-N bond, whereas the C≡N bond might be regarded as a spectator. Nonetheless, multiple quanta of excitation of the C≡N stretch are observed in all of the solvents investigated although the recombination favours $\nu_1 = 0$ (**Table 3**). The UV photolysis of ICN produces < 10% CN(v=1),[18] which cannot account for the ~40% of INC products initially excited in the C≡N stretching mode. The Landau-Teller vibrational cooling model appears to apply consistently across all solvents despite faster vibrational cooling in acetonitrile ($\tau_{1\rightarrow0}$ = 300 ps), which is a polar solvent with hydrogen bonding propensity, than in DCM ($\tau_{1\rightarrow0}$ = 660 ps) and chloroform ($\tau_{1\rightarrow0}$ = 1400 ps).

3.5 CN Reactions with the Solvent

The decline in intensity of free and solvated CN bands in the TEAS data (Section 3.2), and the growth of features assigned to HCN and other species observed in the TVAS data (Section 3.3) indicate that many of the photolytically generated CN radicals react with the solvent. Two

types of reaction are observed: H-atom abstraction from solvent to make HCN, and addition of CN radicals to solvent molecules to form radical adducts. The radical adduct pathway is significant in acetonitrile and is considered in greater detail in a separate publication.[69] Here, we focus on the HCN-forming channel.

Table 4: Single and Double Exponential Time Constants for Growth in Intensity of Product Bands Corresponding to HCN and the Addition Products Observed at 2036 cm^{-1} in Acetonitrile and 2012 cm^{-1} in d-Acetonitrile.

Solvent	**Time Constant / ps**	
	HCN formation	Radical Adduct formation [(a)]
Acetonitrile	73 ± 17	7 ± 3, 33 ± 4
d-Acetonitrile		10.9 ± 3.5, 32 ± 5
Chloroform	700 ± 90	
Dichloromethane	900 ± 120	
Tetrahydrofuran	15 ± 2	

(a) Two time constants are quoted for the growth of the radical adduct; the first accounts for the delayed onset of the radical adduct species.

3.5.1 Reaction of CN Radicals with Dichloromethane

The spectra obtained in the C≡N stretching region following ICN photolysis in DCM solution, shown in **Fig. 4(d)**, were supplemented by spectra of the type we have reported previously in the C-H stretching (ν_3) region around 3260 cm^{-1} for other reactions.[41-42] In this region, C-H stretching excitation shifts the IR absorption bands of HCN by close to -100 cm^{-1} relative to the fundamental band for each additional quantum of vibration. HCN that is vibrationally excited in the C-H mode can therefore be clearly distinguished from ground vibrational level molecules in the TVAS data. TVAS spectra obtained in the C-H stretching region following

267-nm photolysis of ICN in dichloromethane were analysed to obtain the time-dependent band intensities shown in **Figure 6**. These band intensity data were fitted (solid lines in **Fig. 6**) using the kinetic model shown in Scheme II, and the resulting time constants are summarized in **Table 5**. The relative magnitudes of τ_1 and τ_0 imply ~60% branching to HCN (v_3=1). The combined time constant for production of vibrationally excited and ground state HCN (v_3 = 1 and 0) is approximately 20 ps, which is much slower than the decay of the TEAS band assigned to free CN in dichloromethane (1.1 ± 0.5 ps, **Table 1**). Assuming that HCN is not produced more rapidly in vibrational states higher in energy than v_3 = 1, and that the 20 ps time constant therefore corresponds to a timescale of reactive loss of CN radicals, the difference in the two time constants provides further evidence that the CN radicals first form complexes with the solvent. These complexes contribute absorption bands that overlap the I($^2P_{3/2}$) –solvent CT band to form the broad feature peaking at 340 nm in TEA spectra. The single exponential decay time constant extracted for the 340 nm feature of 230 ± 50 ps in DCM (**Table 1**) is much slower than the proposed solvated-CN reaction timescale. However, the decay in intensity of the 340 nm feature can instead be fitted with a double exponential function with time constants of 20 ps and 1 ns (see **Supporting Information**), and the former agrees well with the 20 ps initial growth of all HCN products. The vibrational cooling time constant $\tau_{1\rightarrow0}$ = 160 ± 16 ps extracted from the kinetic fitting of TVAS data to Scheme II is in agreement with the C-H stretching cooling time constant from $v_3 = 1 \rightarrow 0$ of 144 ± 8 ps measured previously using IR-pump IR-probe spectroscopy of HCN in dichloromethane.[58]

Scheme II

$$CN + CH_2Cl_2 \xrightarrow{\tau_1} HCN\ (v_3 = 1) + CHCl_2$$

$$\downarrow \tau_{1\rightarrow0}$$

$$CN + CH_2Cl_2 \xrightarrow{\tau_0} HCN\ (v = 0) + CHCl_2$$

Table 5: Time Constants for Reaction of CN Radicals in Dichloromethane to Produce HCN(v_3=1 and 0) and for Vibrational Relaxation of HCN(v_3=1).

Solvent	**Reaction Time Constant / ps**		**Relaxation Time Constant / ps**
	τ_1	τ_0	$\tau_{1\rightarrow0}$
Dichloromethane	32 ± 3	50 ± 5	160 ± 16

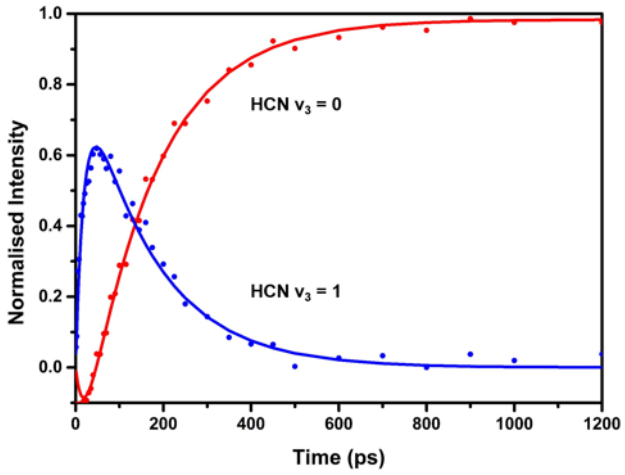

Figure 6: Time-resolved integrated band intensities (dots) and kinetic fits (lines) for TVAS features in the C-H stretching region assigned to HCN(v_3=0) (red) and HCN(v_3=1) (blue) from reaction of CN with CH_2Cl_2. The fits use the model shown in Scheme II.

The C≡N stretching mode of HCN can be observed in the TVAS spectra taken in acetonitrile, chloroform, DCM and THF solutions and is absent in deuterated solvents (see **Figure 4**). The intensity of absorption on the fundamental v_1 C≡N stretching band increases with a time constant that depends strongly on the choice of solvent. The TVAS data suggest that a THF solution favours HCN formation more than do acetonitrile, chloroform and DCM. However, steady state FTIR spectra comparing HCN absorption to ICN depletion indicate a much larger

transition dipole moment of HCN in THF compared to the other solvents, as described in the **Supporting Information**. The magnitude of the HCN TVAS absorption at a time delay of 1300 ps after ICN photolysis in acetonitrile solutions is about eight times smaller, relative to the ICN depletion, than is observed by steady state FTIR spectroscopy of the sample after the TVAS experiments have concluded. This disparity indicates a slower formation process for HCN following ICN photolysis in acetonitrile than is seen in the ps-regime TVAS experiments. The possibility of formation of $C_3H_3N_2^{\bullet}$ radical adducts by addition of CN to acetonitrile was discussed in section 3.2. These adducts are labile free radicals, and hence are not observed by their 2036 cm^{-1} band in steady state FTIR spectra. Instead, decomposition or further reactions may convert these radicals to HCN on nanosecond or longer timescales.

The TVA spectra obtained in both the C≡N and C-H stretching regions show that the growth of the fundamental HCN bands is preceded by a delay in all the solvents studied. This delayed onset is indicative of an intermediate species populated by the CN + solvent reaction that evolves into ground state HCN. On the basis of the evidence presented above from spectra obtained in the C-H stretching spectral region for dichloromethane solutions, negative intensities observed at the HCN v=0 absorption position at early times, and our previous studies of exothermic CN radical reactions in solution,[41-42, 48, 51-52, 57-58] we identify this intermediate species as vibrationally excited HCN. The transition states for reactions of the type CN + RH $\rightarrow$ HCN + R are early on the reaction path,[57] and the H-atom transfer typically liberates about 100 kJ mol^{-1} of energy; both of these factors favour energy flow to the newly forming C-H bond in HCN. **Table 4** summarizes the time constants for the exponential phase of the growth in the HCN 1_0^1 band intensities in different solvents. In THF and acetonitrile, strong coupling of the HCN vibrational modes to the solvent bath causes rapid growth in the intensity of the HCN bands corresponding to absorption by vibrationally ground state HCN molecules. This growth in fundamental band intensities may be limited by the reaction step, or the vibrational

relaxation timescale, or a mixture of the two. However, in DCM and chloroform the solute-solvent coupling is weaker and the vibrational relaxation time constants are significantly larger. Consequently, the timescale for growth of the HCN population is dominated by the vibrational relaxation. The reciprocals of the time constants for HCN growth in the chlorinated solvents presented in **Table 4** are first order rate coefficients for the vibrational relaxation and depend on the coupling of the HCN vibrational motion to the degrees of freedom of the surrounding solvent bath. At early times, this vibrational relaxation might also be influenced by the proximity of the HCN to the radical co-product of reaction which can act as an acceptor for excess vibrational energy.[48]

One apparent anomaly emerges from comparisons of HCN v=0 formation in dichloromethane solutions observed by TVAS in the C≡N and C-H stretching regions: the respective time constants for vibrational cooling of $\tau_{1\rightarrow0}$ = 900 ± 120 ps and $\tau_{1\rightarrow0}$ = 160 ± 16 ps are significantly different. This disparity can be understood if both C-H and C≡N stretching modes of HCN are excited, in which case the different time constants must indicate different coupling of the two vibrational modes of HCN to the solvent bath. A Polanyi-type picture of the reaction dynamics suggests that the location of the transition state favours energy flow into the nascent C-H bond while the C≡N bond plays a spectator role and will be unexcited.[72-73] This simple picture of the dynamics appears to hold in the gas-phase, but may be modified in solution so that the reaction dynamics also promote excitation of the C≡N bond. Alternatively, our observations may indicate that internal vibrational redistribution couples energy from the C-H stretching mode to the C≡N mode on timescales competitive with the vibrational quenching. However the anharmonic coupling between the C-H and C≡N stretching vibrations is too weak (x_{13} = -14.9 cm^{-1})[70] to account for energy flow between these modes on such short timescales unless the presence of the solvent enhances the intramolecular vibrational redistribution of energy.

3.5.2 Reaction of CN Radicals with Tetrahydrofuran

If vibrationally hot HCN formation is a general phenomenon for reactions of CN radicals in organic solvents, these vibrationally excited molecules should contribute to the bands observed in the C≡N stretching region in all the TVAS data reported in Section 3.3 and shown in **Figure 4**. Moreover, the vibrational hot bands should be observed regardless of whether the HCN is excited in the C-H or C≡N stretching mode, or both. These absorption bands will be shifted to lower wavenumber than the fundamental bands by amounts that place them either underneath the INC bands or between the INC and HCN fundamental bands; the relevant anharmonic couplings for the ν_1 C≡N stretching mode in gas phase HCN were listed in Section 3.3. The hot bands are therefore difficult to distinguish unambiguously in the spectral data in acetonitrile, DCM and chloroform. However, as was mentioned in Section 3.3, in THF solution the significantly greater intensity of HCN absorption in the CN region relative to INC enables direct observation of the vibrational cooling of the initially internally excited HCN. The assignment that best accounts for the observed bands on the basis of the (gas-phase) vibrational anharmonicities is to HCN that is excited in the ν_1 C≡N stretch. We therefore assume this assignment in the discussion that follows, but bear in mind that the HCN is also likely to be C-H stretch excited on the basis of evidence from spectra obtained in the 3260 cm^{-1} region in other solvents.

The contribution from HCN 1_1^2 absorption in TVA spectra obtained in THF can be observed despite overlapping the INC 1_0^1 fundamental band because the two features have significantly different time dependences. A Gaussian function centred at 2060 cm^{-1} captures the intensity of both the HCN 1_1^2 and INC 1_0^1 features; on the assumption that a single exponential describes the growth of the INC 1_0^1 component in the kinetic model, the kinetics of the vibrationally hot

HCN can also be extracted. The model in Scheme III was used to analyse the data in terms of vibrational cooling of the C≡N stretch of HCN and parallel formation of INC in the vibrational ground state; the fits of time-dependent band intensities to this model are shown in **Figure 7**. Multiple absorption features prevent extraction of reliable intensities for the HCN 1_2^3 absorption from the spectra presented in **Fig. 4(f)** without imposing some constraints. A Gaussian function centred at 2035 cm^{-1} representing INC 1_1^2 was therefore included in the spectral decomposition and constrained to grow and decay with 15 ps and 30 ps exponential time constants respectively. The ratio of these two time constants was chosen by assuming Landau-Teller type vibrational cooling is the dominant process, while the 30 ps time constant best fitted the exponential growth of the INC 1_0^1 absorption. A Gaussian function centred at 2039 cm^{-1} then captured the intensities assigned to HCN 1_2^3 absorption, and the corresponding kinetics of the nascent HCN are included in **Figure 7** and in the kinetic fits.

Scheme III

$$\text{CN + THF} \xrightarrow{\tau_2} \text{HCN } (v_1 = 2) + \text{THF [-H]}$$

$$\downarrow \tau_{2\rightarrow1}$$

$$\text{CN + THF} \xrightarrow{\tau_1} \text{HCN } (v_1 = 1) + \text{THF[-H]}$$

$$\downarrow \tau_{1\rightarrow0}$$

$$\text{CN + THF} \xrightarrow{\tau_0} \text{HCN } (v = 0) + \text{THF [-H]}$$

$$\text{I + CN or INC } (v > 0) \xrightarrow{\tau_{INC}} \text{INC } (v = 0)$$

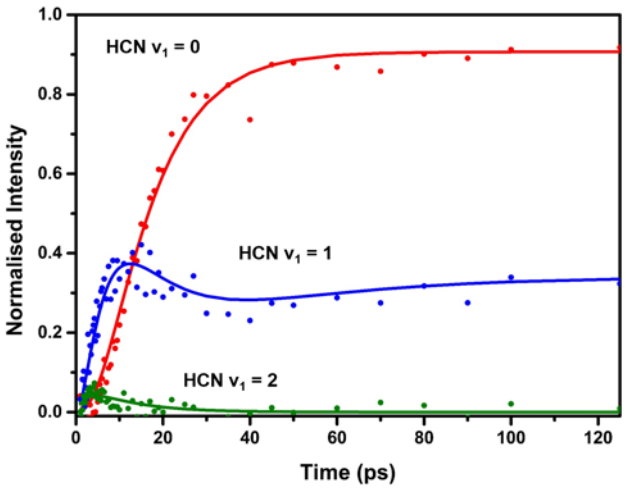

Figure 7: Fits (solid lines) to the experimental measurements (dots) of bands centred at 2039 cm^{-1} (green, HCN v_1=3 ← v_1=2), 2060 cm^{-1} (blue, INC v_1=1 ← v_1=0 and HCN v_1=2 ← v_1=1) and 2080 cm^{-1} (red, HCN v_1=1 ← v_1=0) observed in TVAS spectra following UV photolysis of ICN in THF. An example set of spectra is shown in **Fig. 4(f)**. The fits incorporate production and vibrational cooling of HCN(v_1) and formation of ground state INC, as shown in Scheme III.

Time constants for reaction to make HCN(v_1 = 2, 1 and 0) directly, and for vibrational relaxation, are presented in **Table 6** for experiments in THF. Branching ratios to the HCN(v_1) levels depend inversely on the associated time constants, which are determined from the time-dependent absorption amplitudes. The data in **Table 6** therefore indicate similar yields of these three vibrational levels from the chemical reaction. This excitation in the C≡N stretch cannot simply be a consequence of vibrational adiabaticity in reactions of CN(v=1) because fewer than 10% of the CN radicals from ICN photolysis are vibrationally excited.[18] The cooling of the C≡N stretch of HCN in THF solution is faster than in acetonitrile and substantially faster than in chlorinated solvents. Rose *et al.*[41] measured the v_1 relaxation rate of HCN in THF using IR-pump and IR-probe spectroscopy, but were unable to make the corresponding measurement for the v_3 C-H stretching mode because of spectral overlap with C-H stretching bands of the solvent. They reported a time constant for v_1 = 1 → 0 cooling of 4.7 ± 1.0 ps that is in good agreement with the value of 4.8 ± 1.0 ps deduced from the current analysis. In 3.0 M solutions

of THF in $CDCl_3$ and CD_2Cl_2, Rose *et al*. also found that the time constants for HCN $v_1 = 1 \rightarrow 0$ relaxation were 3.2 ± 0.4 and 3.1 ± 0.2 ps respectively, whereas those for HCN $v_3 = 1 \rightarrow 0$ relaxation (of the C-H stretching mode) were 7.0 ± 0.5 and 7.4 ± 0.8 ps. Comparison with the time constant for HCN $v=1 \rightarrow 0$ relaxation reported in **Table 6** provides further evidence that the excitation we observe in the current TVAS measurements is correctly assigned to the C≡N vibrational mode.

Table 6: Time Constants for the Reaction of CN Radicals with THF to Form Specific Vibrational Levels of HCN, Vibrational Relaxation Steps, and Formation of Vibrationally Ground State INC, Obtained from Fits to the Kinetic Model of Scheme III.

	Reaction Time Constant / ps [(a)]			**Relaxation Time Constant / ps [(a)]**		**INC Time Constant / ps**
	τ_2	τ_1	τ_0	$\tau_{2\rightarrow1}$	$\tau_{1\rightarrow0}$	τ_{INC}
Tetrahydrofuran	31 ± 6	35 ± 7	32 ± 6	2.4 ± 0.5	4.8 ± 1.0	30 ± 10

(a) For the v_1 mode of HCN.

CONCLUSIONS

We report time-resolved UV/visible and infrared absorption spectra that provide a detailed picture of the competing fates of CN radicals produced on timescales of ~100 fs following photolysis of ICN in organic solvents. The combination of electronic and vibrational spectroscopy methods affords a much more complete picture than can be obtained from either of the methods alone. The various destinies of the CN radicals are geminate recombination to ICN and the isomer INC, formation of solvent-radical complexes, and bimolecular reactions with solvent molecules. Evidence is presented that some of the INC geminate recombination products are vibrationally excited in the v_1 C≡N stretching mode, and cool to the ground vibrational level with relaxation time constants that are in a ratio consistent with the

expectations of Landau-Teller theory. Two types of bimolecular reaction are observed: in chloroform, DCM and THF solutions, the dominant reaction with the solvent is an H-atom transfer to make HCN and a solvent[-H] radical, whereas in acetonitrile the CN radical preferentially adds to either the C or N end of the nitrile group.

The bimolecular reactions with solvent molecules make vibrationally excited HCN, which relaxes with a time constant that depends on the coupling of the HCN internal degrees of freedom with solvent modes. Observation of the HCN from CN + dichloromethane reaction, using spectra obtained in the C-H stretching (ν_3) region, unambiguously demonstrates that the chemical dynamics favours HCN (ν_3=1) over vibrationally ground state products. However, incommensurate vibrational relaxation rates obtained in this and the C≡N stretching (ν_1) region indicate that some of the HCN molecules are also, or instead, excited with one or more quanta of the lower frequency ν_1 mode. Excited vibrational levels of this mode may be populated directly from the reaction, or by solvent-promoted internal vibrational energy redistribution from the ν_3 mode.

These studies of the chemical dynamics that follow ICN photolysis in various organic solvents provide benchmark information against which the observed dynamics of reactions with added co-solutes can be compared. They also demonstrate the substantial effect that the choice of organic solvent can have on the chemical processes that follow homolytic cleavage of covalent bonds in solute molecules.

ACKNOWLEDGEMENTS

MPG acknowledges award of a Marie Curie International Incoming Fellowship (PIIF-GA-2012-326988). The Bristol group thanks the European Research Council (ERC, Advanced Grant 290966 CAPRI) for financial support. The ULTRA Laser Facility is supported by the

Science and Technology Facilities Council (STFC, Facility Grant ST/501784). We are grateful to Ian P. Clark, Paul M. Donaldson and Mike Towrie (STFC Rutherford Appleton Laboratory) for assistance with the experimental measurements.

SUPPORTING INFORMATION AVAILABLE

All experimental data are archived in the University of Bristol's Research Data Storage Facility (DOI 10.5523/bris.1ibpp456fas8v1tgycjl8ex43i). The Supporting Information contains summaries of DFT and TD-DFT calculations of structrues and spectra of CN-solvent complexes, TEA spectra of BrCN in acetonitrile, FTIR spectra of solutions obtained following ICN photolysis in acetonitrile, THF and DCM, and time constants for INC geminate recombination. This information is available free of charge via the internet at http://pubs.acs.org.

REFERENCES

1. Dantus, M.; Rosker, M. J.; Zewail, A. H. Femtosecond Real-Time Probing of Reactions 2. The Dissociation Reaction of ICN. *J Chem Phys* **1988,** *89*, 6128-6140.
2. Roberts, G.; Zewail, A. H. Femtosecond Real-Time Probing of Reactions 7. A Quantum and Classical Mechanical Study of the ICN Dissociation Experiment. *J Phys Chem-Us* **1991,** *95*, 7973-7993.
3. Scherer, N. F.; Knee, J. L.; Smith, D. D.; Zewail, A. H. Femtosecond Photofragment Spectroscopy - the Reaction ICN → CN+I. *J Phys Chem-US* **1985,** *89*, 5141-5143.
4. Amatatsu, Y.; Yabushita, S.; Morokuma, K. Ab-Initio Potential-Energy Surfaces and Trajectory Studies of A-Band Photodissociation Dynamics - ICN* → I+CN and I*+CN. *J Chem Phys* **1994,** *100*, 4894-4909.
5. Qian, J. W.; Tannor, D. J.; Amatatsu, Y.; Morokuma, K. Ab-Initio Structure and Wave-Packet Dynamics of ICN Photodissociation. *J Chem Phys* **1994,** *101*, 9597-9609.
6. Yabushita, S.; Morokuma, K. Ab Initio Potential-Energy Surfaces for Rotational-Excitation of CN Product in the A-Band Photodissociation of ICN. *Chem Phys Lett* **1990,** *175*, 518-524.

7. Baronavski, A. P.; Mcdonald, J. R. Electronic, Vibrational and Rotational Energy Partitioning of CN Radicals from Laser Photolysis of ICN at 266 nm. *Chem Phys Lett* **1977,** *45*, 172-176.
8. Black, J. F.; Hasselbrink, E.; Waldeck, J. R.; Zare, R. N. Photofragment Orientation as a Probe of near-Threshold Nonadiabatic Phenomena in the Photodissociation of ICN. *Mol Phys* **1990,** *71*, 1143-1153.
9. Black, J. F.; Waldeck, J. R.; Zare, R. N. Evidence for 3 Interacting Potential-Energy Surfaces in the Photodissociation of ICN at 249 nm. *J Chem Phys* **1990,** *92*, 3519-3538.
10. Bowman, J. M.; Mayrhofer, R. C.; Amatatsu, Y. Coupled-Channel Scattering Calculations of ICN(Ã–X̃) Photodissociation Using Ab-Initio Potentials. *J Chem Phys* **1994,** *101*, 9469-9479.
11. Chang, J. L.; Chen, K. M.; Lin, W. Y.; Chen, Y. T. Study of Photodissociation Dynamics Using Sub-Doppler Fluorescence Imaging Method: Photodissociation of ICN at 308 nm. *J Chin Chem Soc-Taip* **2001,** *48*, 619-624.
12. Chen, K.; Kuo, C.; Tzeng, M.; Shian, M.; Chung, S. E. Imaging Photofragments in Velocity Space by Laser Sheet Illumination Techniques - Photodissociation of ICN. *Chem Phys Lett* **1994,** *221*, 341-346.
13. Chen, K. M.; Chen, K. C.; Yang, T. H. Quantum Theory of ICN Photodissociation: Density Matrices of Photofragments from a Parallel Transition. *J Chinese Chem Soc* **2007,** *54*, 149-156.
14. Coronado, E. A.; Batista, V. S.; Miller, W. H. Nonadiabatic Photodissociation Dynamics of ICN in the Ã Continuum: A Semiclassical Initial Value Representation Study. *J Chem Phys* **2000,** *112*, 5566-5575.
15. Costen, M. L.; North, S. W.; Hall, G. E. Vector Signatures of Adiabatic and Diabatic Dynamics in the Photodissociation of ICN. *J Chem Phys* **1999,** *111*, 6735-6749.
16. Dugan, C. H.; Anthony, D. The Origin of Fragment Rotation in ICN Photodissociation. *J Phys Chem-US* **1987,** *91*, 3929-3932.
17. Dzegilenko, F. N.; Bowman, J. M.; Amatatsu, Y. Non-Condon Effects in Photodissociation of ICN(Ã –X̃): Coupled-Channel Scattering Calculations. *Chem Phys Lett* **1997,** *264*, 24-30.
18. Fisher, W. H.; Eng, R.; Carrington, T.; Dugan, C. H.; Filseth, S. V.; Sadowski, C. M. Photodissociation of BrCN and ICN in the A Continuum - Vibrational and Rotational Distributions of CN($X^2\Sigma^+$). *Chem Phys* **1984,** *89*, 457-471.
19. Griffiths, J. A.; Elsayed, M. A. The Photodissociation Dynamics of ICN at 304.67 nm by State-Selective One-Dimensional Translational Fragmentation Spectroscopy. *J Chem Phys* **1994,** *100*, 4910-4916.
20. Guo, H.; Schatz, G. C. Nonadiabatic Effects in Photodissociation Dynamics - a Quantum-Mechanical Study of ICN Photodissociation in the A Continuum. *J Chem Phys* **1990,** *92*, 1634-1642.
21. Hall, G. E.; Sivakumar, N.; Houston, P. L. Rotational Alignment of the CN Fragment of ICN Photodissociation. *J Chem Phys* **1986,** *84*, 2120-2128.
22. Hancock, G.; Richmond, G.; Ritchie, G. A. D.; Taylor, S.; Costen, M. L.; Hall, G. E. Frequency Modulated Circular Dichroism Spectroscopy: Application to ICN Photolysis. *Mol Phys* **2010,** *108*, 1083-1095.
23. Hasselbrink, E.; Waldeck, J. R.; Zare, R. N. Orientation of the CN $X^2\Sigma^+$ Fragment Following Photolysis of ICN by Circularly Polarized-Light. *Chem Phys* **1988,** *126*, 191-200.
24. Joswig, H.; O'Halloran, M. A.; Zare, R. N.; Child, M. S. Photodissociation Dynamics of ICN - Unequal Population of the CN $X^2\Sigma^+$ Fine-Structure Components. *Faraday Discuss* **1986,** *82*, 79-88.

25. Lambert, M.; Callen, B.; Dugan, H.; Filseth, S. V.; Morgan, F. J.; Sadowski, C. M. ICN Photodissociation at 193 nm - CN($B^2\Sigma$) Rotational Distributions and Fluorescence Polarization. *Chem Phys Lett* **1987,** *139*, 45-48.
26. Li, R. J.; McGivern, W. S.; North, S. W. Temperature-Dependent Photodissociation Dynamics of ICN at 262 nm. *Chem Phys Lett* **2001,** *334*, 47-54.
27. Marinelli, W. J.; Sivakumar, N.; Houston, P. L. Photodissociation Dynamics of Nozzle-Cooled ICN. *J Phys Chem-Us* **1984,** *88*, 6685-6692.
28. Nadler, I.; Mahgerefteh, D.; Reisler, H.; Wittig, C. The 266 nm Photolysis of ICN - Recoil Velocity Anisotropies and Nascent E,V,R,T Excitations for the CN + I($^2P_{3/2}$) and CN + I($^2P_{1/2}$) Channels. *J Chem Phys* **1985,** *82*, 3885-3893.
29. Nadler, I.; Reisler, H.; Wittig, C. Energy Disposal in the Laser Photodissociation of ICN and BrCN at 300K and in a Free Jet Expansion. *Chem Phys Lett* **1984,** *103*, 451-457.
30. North, S. W.; Mueller, J.; Hall, G. E. Vector Correlations in the 308 nm Photodissociation of ICN. *Chem Phys Lett* **1997,** *276*, 103-109.
31. Pitts, W. M.; Baronavski, A. P. Wavelength Dependence of the I($5^2P_{1/2,3/2}$) Branching Ratio from ICN Ã State Photolysis. *Chem Phys Lett* **1980,** *71*, 395-399.
32. Sabetydzvonik, M. J.; Cody, R. J. Internal State Distribution of CN Free-Radicals Produced in Photodissociation of ICN. *J Chem Phys* **1977,** *66*, 125-135.
33. Shokoohi, F.; Hay, S.; Wittig, C. Spin-Aligned CN($X^2\ \Sigma^+$) from the Photodissociation of ICN and BrCN. *Chem Phys Lett* **1984,** *110*, 1-6.
34. Suzuki, T.; Ebata, T.; Anezaki, Y.; Mikami, N.; Ito, M. Rotational Distribution of CN Fragment Produced by the 266 nm Photolysis of ICN in a Supersonic Free Jet. *Chem Lett* **1984,** *13*, 1177-1180.
35. Wei, H.; Carrington, T. A Time-Dependent Calculation of the Alignment and Orientation of the CN Fragment of the Photodissociation of ICN. *J Chem Phys* **1996,** *105*, 141-155.
36. Benjamin, I.; Wilson, K. R. Proposed Experimental Probes of Chemical-Reaction Molecular-Dynamics in Solution - ICN Photodissociation. *J Chem Phys* **1989,** *90*, 4176-4197.
37. Wan, C. Z.; Gupta, M.; Zewail, A. H. Femtochemistry of ICN in Liquids: Dynamics of Dissociation, Recombination and Abstraction. *Chem Phys Lett* **1996,** *256*, 279-287.
38. Moskun, A. C.; Bradforth, S. E. Photodissociation of ICN in Polar Solvents: Evidence for Long Lived Rotational Excitation in Room Temperature Liquids. *J Chem Phys* **2003,** *119*, 4500-4515.
39. Rivera, C. A.; Winter, N.; Harper, R. V.; Benjamin, I.; Bradforth, S. E. The Dynamical Role of Solvent on the ICN Photodissociation Reaction: Connecting Experimental Observables Directly with Molecular Dynamics Simulations. *Phys. Chem. Chem. Phys.* **2011,** *13*, 8269-8283.
40. Larsen, J.; Madsen, D.; Poulsen, J. A.; Poulsen, T. D.; Keiding, S. R.; Thogersen, J. The Photoisomerization of Aqueous ICN Studied by Subpicosecond Transient Absorption Spectroscopy. *J Chem Phys* **2002,** *116*, 7997-8005.
41. Rose, R. A.; Greaves, S. J.; Abou-Chahine, F.; Glowacki, D. R.; Oliver, T. A. A.; Ashfold, M. N. R.; Clark, I. P.; Greetham, G. M.; Towrie, M.; Orr-Ewing, A. J. Reaction Dynamics of CN Radicals with Tetrahydrofuran in Liquid Solutions. *Phys. Chem. Chem. Phys.* **2012,** *14*, 10424-10437.
42. Rose, R. A.; Greaves, S. J.; Oliver, T. A. A.; Clark, I. P.; Greetham, G. M.; Parker, A. W.; Towrie, M.; Orr-Ewing, A. J. Vibrationally Quantum-State-Specific Dynamics of the Reactions of CN Radicals with Organic Molecules in Solution. *J Chem Phys* **2011,** *134*, 244503.

43. Benjamin, I. Photodissociation of ICN in Liquid Chloroform - Molecular-Dynamics of Ground and Excited-State Recombination, Cage Escape, and Hydrogen Abstraction Reaction. *J Chem Phys* **1995,** *103*, 2459-2471.
44. Johnson, M. L.; Benjamin, I. Photodissociation of ICN at the Water/Chloroform Interface. *J Phys Chem A* **2009,** *113*, 7403-7411.
45. Vieceli, J.; Chorny, I.; Benjamin, I. Photodissociation of ICN at the Liquid/Vapor Interface of Chloroform. *J Chem Phys* **2001,** *115*, 4819-4828.
46. Winter, N.; Benjamin, I. Photodissociation of ICN at the Liquid/Vapor Interface of Water. *J Chem Phys* **2004,** *121*, 2253-2263.
47. Winter, N.; Chorny, I.; Vieceli, J.; Benjamin, I. Molecular Dynamics Study of the Photodissociation and Photoisomerization of ICN in Water. *J Chem Phys* **2003,** *119*, 2127-2143.
48. Glowacki, D. R.; Rose, R. A.; Greaves, S. J.; Orr-Ewing, A. J.; Harvey, J. N. Ultrafast Energy Flow in the Wake of Solution-Phase Bimolecular Reactions. *Nat. Chem.* **2011,** *3*, 850-855.
49. Moskun, A. C.; Jailaubekov, A. E.; Bradforth, S. E.; Tao, G. H.; Stratt, R. M. Rotational Coherence and a Sudden Breakdown in Linear Response Seen in Room-Temperature Liquids. *Science* **2006,** *311*, 1907-1911.
50. Fraenkel, R.; Haas, Y. Photolysis of ICN in a Cryogenic Matrix. *Chem Phys Lett* **1993,** *214*, 234-240.
51. Orr-Ewing, A. J. Bimolecular Chemical Reaction Dynamics in Solution. *J Chem Phys* **2014,** *140*, 090901.
52. Orr-Ewing, A. J. Dynamics of Bimolecular Reactions in Solution. *Annu. Rev. Phys. Chem.* **2015,** *66*, 119-141.
53. Voth, G. A.; Hochstrasser, R. M. Transition State Dynamics and Relaxation Processes in Solutions: A Frontier of Physical Chemistry. *J Phys Chem-US* **1996,** *100*, 13034-13049.
54. Raftery, D.; Gooding, E.; Romanovsky, A.; Hochstrasser, R. M. Vibrational Product State Dynamics in Solution-Phase Bimolecular Reactions - Transient Infrared Study of CN Radical Reactions. *J Chem Phys* **1994,** *101*, 8572-8579.
55. Crowther, A. C.; Carrier, S. L.; Preston, T. J.; Crim, F. F. Time-Resolved Studies of CN Radical Reactions and the Role of Complexes in Solution. *J Phys Chem A* **2008,** *112*, 12081-12089.
56. Crowther, A. C.; Carrier, S. L.; Preston, T. J.; Crim, F. F. Time-Resolved Studies of the Reactions of CN Radical Complexes with Alkanes, Alcohols, and Chloroalkanes. *J Phys Chem A* **2009,** *113*, 3758-3764.
57. Glowacki, D. R.; Orr-Ewing, A. J.; Harvey, J. N. Product Energy Deposition of CN + Alkane H Abstraction Reactions in Gas and Solution Phases. *J Chem Phys* **2011,** *134*, 214508.
58. Greaves, S. J.; Rose, R. A.; Oliver, T. A. A.; Glowacki, D. R.; Ashfold, M. N. R.; Harvey, J. N.; Clark, I. P.; Greetham, G. M.; Parker, A. W.; Towrie, M., et al. Vibrationally Quantum-State-Specific Reaction Dynamics of H Atom Abstraction by CN Radical in Solution. *Science* **2011,** *331*, 1423-1426.
59. Greetham, G. M.; Burgos, P.; Cao, Q.; Clark, I. P.; Codd, P. S.; Farrow, R. C.; George, M. W.; Kogimtzis, M.; Matousek, P.; Parker, A. W., et al. ULTRA: A Unique Instrument for Time-Resolved Spectroscopy. *Appl. Spectrosc.* **2010,** *64*, 1311-1319.
60. Roberts, G. M.; Marroux, H. J. B.; Grubb, M. P.; Ashfold, M. N. R.; Orr-Ewing, A. J. On the Participation of Photoinduced N-H Bond Fission in Aqueous Adenine at 266 and 220 nm: A Combined Ultrafast Transient Electronic and Vibrational Absorption Spectroscopy Study. *J Phys Chem A* **2014,** *118*, 11211-11225.

61. Grubb, M. P.; Orr-Ewing, A. J.; Ashfold, M. N. R. KOALA: A New Program for the Processing and Decomposition of Transient Spectra. *Rev. Sci. Instrumen.* **2014,** *84*, 064104.
62. Felps, W. S.; Rupnik, K.; Mcglynn, S. P. Electronic Spectroscopy of the Cyanogen Halides. *J Phys Chem-US* **1991,** *95*, 639-656.
63. Hess, W. P.; Leone, S. R. Absolute I* Quantum Yields for the ICN A-State by Diode-Laser Gain-vs-Absorption Spectroscopy. *J Chem Phys* **1987,** *86*, 3773-3780.
64. Pieniazek, P. A.; Bradforth, S. E.; Krylov, A. I. Spectroscopy of the Cyano Radical in an Aqueous Environment. *J Phys Chem A* **2006,** *110*, 4854-4865.
65. Frisch, M. J.; Trucks, G. W.; Schlegel, H. B.; Scuseria, G. E.; Robb, M. A.; Cheeseman, J. R.; Scalmani, G.; Barone, V.; Mennucci, B.; Petersson, G. A., et al. *Gaussian 09*, Gaussian Inc., Wallingford CT, 2009.
66. Dunning, G. T.; Preston, T. J.; Greaves, S. J.; Greetham, G. M.; Clark, I. P.; Orr-Ewing, A. J. Vibrational Excitation of Both Products of the Reaction of CN Radicals with Acetone in Solution. *J Phys Chem A* **2015**. DOI: 10.1021/acs.jpca.5b05624
67. *NIST-JANAF Thermochemistry Table, NIST Standard Reference Database Number 13*. 2013.
68. Samuni, U.; Kahana, S.; Fraenkel, R.; Haas, Y.; Danovich, D.; Shaik, S. The ICN-INC System - Experiment and Quantum-Chemical Calculations. *Chem Phys Lett* **1994,** *225*, 391-397.
69. Koyama, D.; Coulter, P.; Grubb, M. P.; Greetham, G. M.; Clark, I. P.; Orr-Ewing, A. J. Reaction Dynamics of CN Radicals in Acetonitrile Solutions. *submitted* **2015**.
70. Smith, A. M.; Coy, S. L.; Klemperer, W.; Lehmann, K. K. Fourier-Transform Spectra of Overtone Bands of HCN from 5400 to 15100 cm^{-1}. *J Mol Spectrosc* **1989,** *134*, 134-153.
71. Owrutsky, J. C.; Raftery, D.; Hochstrasser, R. M. Vibrational-Relaxation Dynamics in Solutions. *Annu. Rev. Phys. Chem.* **1994,** *45*, 519-555.
72. Polanyi, J. C. Concepts in Reaction Dynamics. *Acc. Chem. Res.* **1972,** *5*, 161-168.
73. Raphael D. Levine, R. B. B. *Molecular Reaction Dynamics and Chemical Reactivity*. Oxford University Press: 1987.

TABLE OF CONTENTS GRAPHIC